165 K Microcooler Operating with a Sorption Compressor and a Micromachined Cold Stage

J.F. Burger, H.J. Holland, J.H. Seppenwoolde, E. Berenschot, H.J.M. ter Brake, J.G.E. Gardeniers, M. Elwenspoek and H. Rogalla

University of Twente, Faculty of Applied Physics
P.O. Box 217,7500 AE Enschede, The Netherlands

ABSTRACT

This paper presents the fabrication of a microcooler consisting of small stainless steel sorption compressor cells, micromachined silicon check valves, and a micromachined cold stage that incorporates glass-tube heat exchangers. The design, fabrication and experiments on the different elements are described. Two compressor cells were thermally cycled to investigate the dynamic behaviour. The cold stage could reach a stable temperature of 169 K with a cooling power of about 200 mW.

INTRODUCTION

During recent years a rapid development has taken place of LT-electronics and especially of superconducting devices. However, there exists a gap between this development and the availability of enabling technologies that are essential for the commercialization of LT-electronics[1]. These enabling technologies are low-cost, highly reliable cryogenic refrigeration systems and energy-efficient cryogenic packaging of the LT-electronic device with the cryogenic refrigerators. Much effort is currently put in the development of such reliable and cheap coolers, but typically small systems are still rather large in terms of size (> 1 kg) and cooling power (> 1 W). Low-temperature applications requiring very little cooling power, such as a single chip with a low noise amplifier or a superconducting magnetometer, would benefit from very small closed-cycle coolers. Such coolers do not exist and in this respect it was suggested[3] that micromachining techniques can be attractive for miniature cooler components, such as heat exchangers, check valves or compressors. As a typical example in this respect, this paper presents realized components for a microcooling system, which consists of a sorption compressor with a micromachined cold stage.

The sorption/Joule-Thomson (JT) cycle was identified as a potential candidate for the development of a microminiature cooler aiming at a cooling power in the range of 10 mW at 80K[3]. The advantage of this cycle is the absence of wear-related moving parts, except for some check valves. This facilitates scaling down of the system to very small sizes, it minimizes electromagnetic and mechanical interferences (which is important for many applications), and it

Cryocoolers 11, edited by R.G. Ross, Jr.
Kluwer Academic/Plenum Publishers, 2001

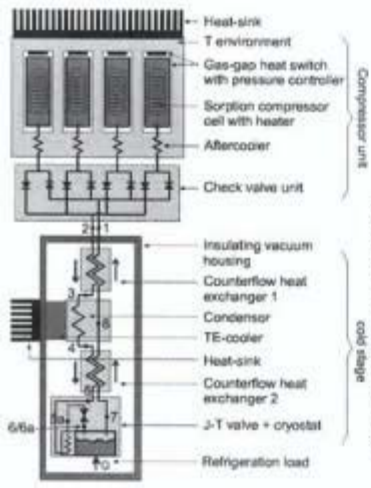

Figure 1. Sorption cooler set-up.

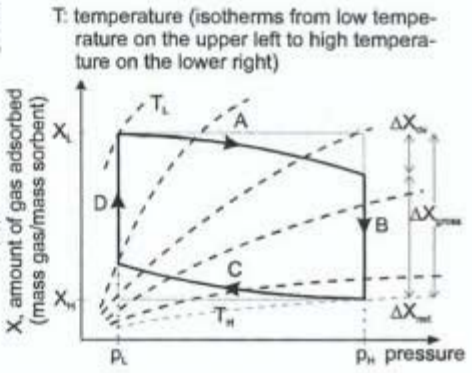

Figure 2. Schematic of compressor cycle

offers the potential of a long life time. The operating principle of sorption coolers is discussed in several publications[4,5], and is briefly summarized below.

A sorption cooler consists of a compressor unit, a counterflow heat exchanger, and a JT expansion valve, see Fig. 1. Compressed gas corning out of the compressor unit is cooled to the environmental temperature after which it is fed into the first counterflow heat exchanger. A (thermoelectric) precooler such as depicted in Fig. 1 may be applied to improve the system performance. Next, the compressed refrigerant is expanded in the JT valve to provide refrigeration. The low pressure refrigerant then returns through the recuperative heat exchangers to the compressor unit. The compressor unit basically contains four sorption cells and several check valves to control the gas flows. Low and high pressures are generated by the cyclic ad- and desorption of a working gas on a sorption material, which is accomplished by cooling and heating of the sorption material. The gas can either be physically adsorbed onto or chemically absorbed into various solids. Usually, heating occurs with an electrical heater and cooling is done with a heat-switch between the sorption cell and a heat sink on the outside (typically a gas-gap switch). A compressor cycle of one cell is schematically shown in Fig. 2. The cell is heated during sections A and B, and cooled during C and D. During sections A and C both valves of the cell are closed, and the cell is in a regenerating phase. During sections B and D one of the valves is opened; the cell generates a high pressure gas flow out of the cell during B, and a low pressure gas flow into the cell during D. It is important to notice that the valves are passive check valves; the cycle is driven by the temperature induced pressure variations of the compressor cells. In our case, a complete compressor cycle typically takes about 10 minutes.

A thermodynamic analysis of sorption coolers was presented elsewhere[6]. In that analysis the Coefficients of Performance (COP) of the compressor and the cold stage were modelled separately, both for quasi-static conditions. It followed that the compressor performance strongly depends on the sorption material, the gas, the compressor material, and the temperatures and pressures the compressor operates on. Microporous activated carbon with a high internal surface area was chosen as the sorption material for a first demonstrator cooler, in combination with xenon (or alternatively ethylene) as a refrigerant gas that is able to cool to about 165 K. This sorption cooler can be used as a first stage of a two-stage sorption cooler that is able to cool to 80 K. For a low pressure of 1 bar, an optimum compressor performance was found for compression to 10–20 bar and compressor cells operating between 300 and 600 K. However, it

appeared that the cold stage required somewhat higher pressures (> 60 bar) to perform well. It was shown that precooling of the gas by means of a miniature thermoelectric cooler connected somewhere halfway the counterflow heat exchanger results in a dramatic improvement of the performance at a pressure of 20 bar, resulting in an overall cooler performance of about 3%. We aim at a cooling power of 200 mW, requiring a compressor input power of less than 10 W and a xenon massflow of about 2.5 mg/s (or 0.5 mg/s for ethylene). These parameters define the requirements for the individual cooler elements.

SORPTION COMPRESSOR

Requirements. (1) The ratio of the cylinder thermal mass to the sorber thermal mass should be minimal in order to maximize the compressor COP[6]. The cylinder thermal mass includes the thermal mass of the heater, thermocouple and other stainless steel components. These thermal masses should, therefore, be minimal as well. (2) A 300 μm gas-gap heat switch is required between the inner sorption cell and the outer cylinder. Conduction and radiation losses between the inner and outer cylinders should be minimized. Furthermore, the gas-gap vacuum space should be perfectly sealed (all welded) and without any materials that could show outgassing so that it can be reversibly actuated by a metal hydride sorber[7]. (3) The sorption cell should contain highly porous charcoal with a grain size of minimal 200 μm to maintain a low pressure drop over the sorption bed. As a consequence, a filter is required in the gas connection line to keep the sorber material in the cell. (4) The fabrication should be as simple as possible.

Design and realization. Fig. 3a shows a cross-sectional drawing of one sorption compressor cell with integrated gas-gap heat switch. All components are made of stainless steel 316L, except the thermocouple sheath which is made of stainless steel 304. The different components are assembled by laser-welding and high-temperature soldering.

The E-type thermocouple consists of a 250 μm outer diameter stainless steel sheath which contains the two 60 μm thermocouple wires, isolated by a MgO ceramic powder[8]. A thermocouple with a length of 0.5 meter and a total resistance of 380 ohm was coiled and fixed as depicted in Fig. 3a. Long-duration experiments showed that these thermocouples are also suitable to be applied as an isolated heater, so that in fact a combined heater/thermocouple results. In this heater experiment, five thermocouples were cycled 3.10^5 times between 300 K and 600 K with an input power of 30 W; no significant degradation of the heater or thermocouple fucntion was observed.

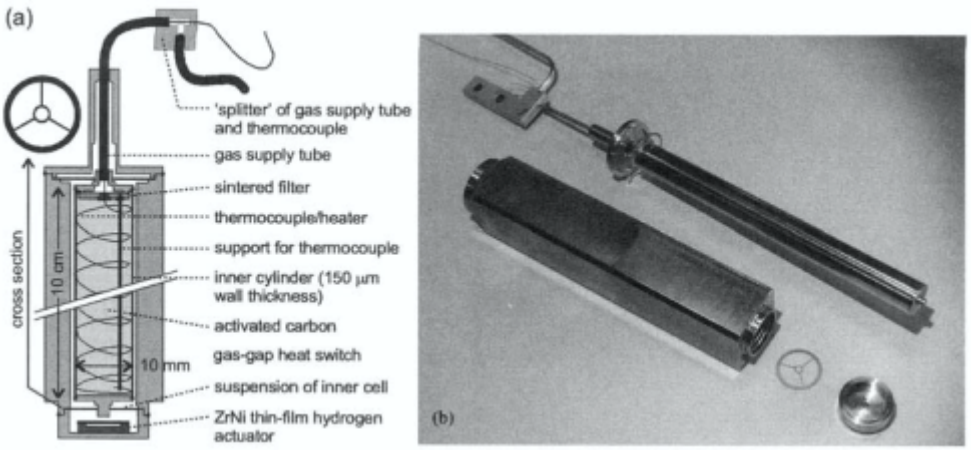

Figure 3. (a) Cross sectional drawing of one sorption compressor cell, (b) Photo's of some elements.

The inner sorption cylinder has a wall thickness of 150 μm and is laser-welded to the end-caps. One end-cap is integrated with the sintered filter (2 μm), the gas supply tube, the thermocouple and its support. The thermocouple is connected to the outside world via the gas supply tube, which reduces the number of feedthroughs through the gas-gap vacuum space. The inner sorption cell is suspended by two 'wheels' with three thin spokes, see Fig. 3a. This construction facilitates accurate radial positioning, longitudinal flexibility to account for thermal expansion differences between both cylinders and low thermal conduction losses between both cylinders. The top closure of the outer cylinder contains an extension to reduce the thermal conduction losses via the longer gas supply tube. The lower closure can be supplied with a thin-film ZrNi hydrogen actuator to control the hydrogen pressure in the gas-gap. In the current version of the compressor that is used for the described experiments, a gas supply in combination with a small vacuum pump is used to control the pressure in the gas gap. Fig. 3b shows photographs of the compressor components and an assembled compressor cell.

Experiments. To study the behaviour of the sorption compressor cells and to compare it with our models, cycling experiments were carried out with a combination of two compressor cells. Fig. 4a shows the experimental set-up that is designed to operate the two cells through ab- and desorption cycles as depicted in Fig. 2, where the two cells are 180 degrees out of phase. The metering valve was used to create the desired flow restriction. A data acquisition system was used to measure and store the following parameters: the electrical input powers, temperatures and pressures of the two sorption cells, the pressures in the two gas-gap heat switches, and the massflow from cell one to two (the sensor could only measure flow in one direction). To run the experiment automatically, the data acquisition system could control the following parameters: the input powers of the two cells, the active valve between the two cells that controls the massflow period, and the active valves that control the pressure in the two gas-gap heat switches. An ethylene gas supply system and a vacuum pump were connected to the system via two valves; in this way the system could be pumped and purged before filling with ethylene gas. Care was taken in minimizing the dead volumes of the system because dead volumes deteriorate the compressor performance[6]. However, the active valve and the massflow sensor still contributed significantly to the dead volume, 30% and 50% of the sorption cell volume, respectively. In a real sorption compressor these components are not present, and a much better performance can be expected.

Fig. 4b shows a typical measurement of the temperatures and pressures in the two cells. Also depicted are the state of the active valve between the cells and the massflow from cell 1 to 2. The measurement clearly shows the alternating periods of the two cells. The phases A-D of Fig. 2 are indicated in Fig. 4b on the pressure-curve of cell 2. The sudden pressure drop and pressure peak of cell 1 are caused by the dead volume of the active valve. Furthermore, it can be seen that the

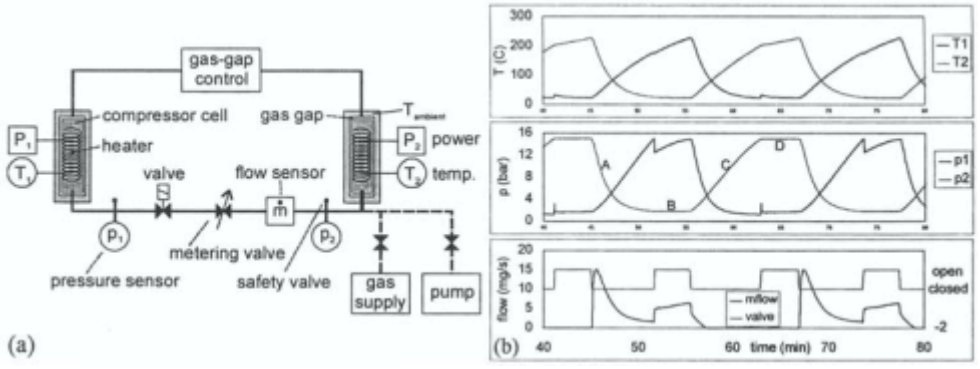

Figure 4. (a) Measurement set-up for flow-tests between two sorption compressor cells, (b) Typical measurement results (see text).

pressure was cycled between 2 and 15 bar instead of the required 1 and 20 bar. The experiments were carried out on a slightly older version of the sorption cell with a NiCr heater wrapped around the cell instead of the more robust thermocouple-heater. The NiCr heater was limited in terms of temperatures and input powers that could be applied. However, the obtained pressures and massflows matched with the modelled values[6], and it is expected that the required pressures can be obtained with the current design of the sorption cells, especially because the extra dead volumes are not present anymore.

CHECK VALVES

Requirements. The requirements for the check valves are derived from the cooler parameter settings as given in the introduction: (1) The valves have to stand periodically pressure differences up to the maximum pressure difference of 20 bar; 50 bar is chosen as a safe limit. (2) Gas leakage in the closed direction is a loss factor and should be kept below a small fraction of the normal gas flow in forward direction (< 1% of 2.5 mg/s). (3) The valve should close immediately as soon as the pressure difference reverses. Consequently, the valve should be normally closed but without a significant spring force to reduce the pressure drop in forward direction. (4) In forward direction, the massflows through the high- and low-pressure valves are the same but the absolute gas pressures and densities are a factor of 20 different. In both cases, the pressure drop should be a small fraction of the absolute pressure. By designing a check valve

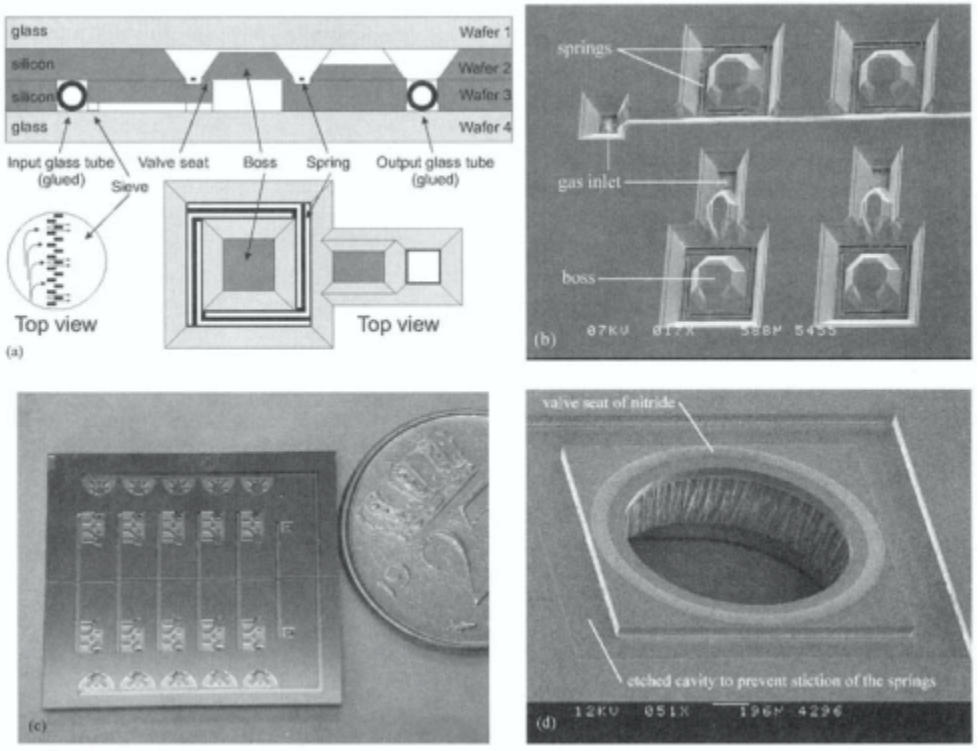

Figure 5. (a) Design impression of the high-pressure check valve. Spring dimensions (height x width x length): **10 x 50 x 1200 μm;** boss: 1 x 1 mm. (b) Photo of top wafer with 4 KOH-etched bosses (part of a 10-valve manifold), (c) Photo of the backside of 2 manifolds with 10 valves, prior to separation of the manifolds and integration with glass-tubes, (d) Photo of a section of the bottom wafer.

that fulfills this requirement for the low-pressure gas, the same valve will certainly also fulfill the requirements for the high-pressure gas. (5) From experiments with a large scale sorption cooler it appeared that leaking check valves (of a commercial type) were the major cause of malfunction of the system[9]. This was explained by contamination of the valve seat. From this we concluded that prevention of possible contamination is a major requirement.

Design and realization. The valve consists of a thick plate (boss) suspended by four thin springs[10], see Fig. 5. The thin springs behave like single clamped beams, thus facilitating high deflections which are required to obtain a low pressure drop in the forward direction. When the valve is in forward direction, the gas is able to flow through the holes surrounding the springs. The entire valve construction, including the interfacing gas lines, is made out of two silicon wafers that are covered by two glass wafers, all bonded together. The design is such that the gas lines on both sides of the valve can cross in the upper and lower wafers. This is required for the construction of an integrated valve manifold that has only six connections to the outside world: four to the compressor cells and two to the cold stage. The valve seat is made out of the polished surface of the wafers, facilitating a perfect fit and alignment of both sides of the valve seat. Stiction of the fragile spring beams to the bottom wafer is prevented by etching a cavity in the bottom wafer under the beams. Stiction or bonding of the valve seat is prevented by application of a nitride coating[11]. The maximum allowed deflection of the boss can be selected by choosing an appropriate thickness of the boss relative to the wafer thickness. A $4\ \mu m$ sieve is constructed in the inflow line of the valve to trap possible contamination. The sieve is made of a row of pillars standing in the channel. Fluidic and mechanical modelling was applied to find the proper dimensions of the valve construction; this is described in more detail elsewhere[10].

Experiments. Experiments with samples bonded with $500\ \mu m$ Pyrex wafers showed that the valves could withstand pressures up to 65 bar in closed direction with a leakage flow that was not detectable ($< 1\ \mu g/s$). At higher pressures, glass wafer 1 burst. Samples bonded with thicker Pyrex wafers were tested up to 125 bar and did not burst at all.

With the valves in forward direction, the pressure drop was measured as a function of the massflow. For an absolute nitrogen pressure of 2 bar and a massflow of 1 mg/s, a pressure drop of approximately 30 mbar was measured. It was shown that this pressure drop was more or less equally divided over the connecting tubes, the filter and the valve itself.

To test the influence of contamination on the closing behaviour of the valve, small particles of $1 - 10\ \mu m$ were blown through a valve without integrated filter. At $\Delta p = 50$ bar a leakage flow was measured of 1.2 mg/s, which is very significant (in the same range as the forward flow). This illustrates the importance to trap contaminant particles in a filter.

Finally, a long duration experiment was done involving many forward/closed switchings. Fig. 6 shows that the leakage flow reduced from an initial 3% to 0.5% of the forward flow after a few thousand cycles. This behaviour is probably caused by a small particle or irregularity in the

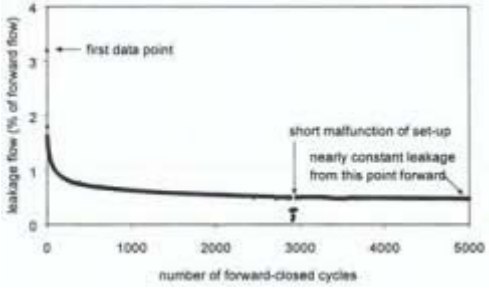

Figure 6. Leakage flow as a function of the number of forward-closed cycles of a valve.

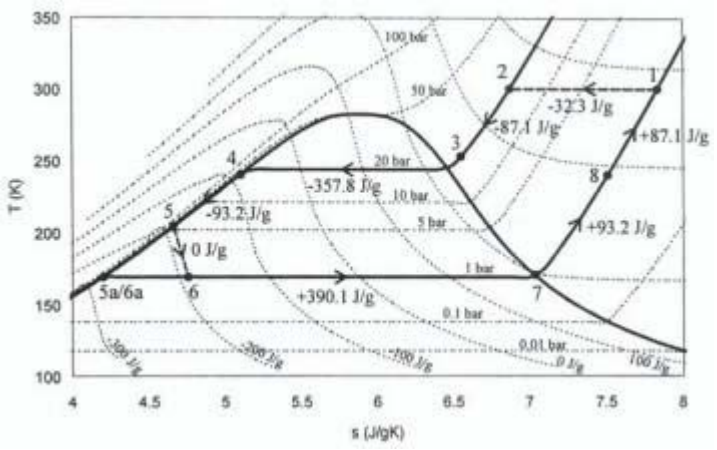

Figure 7. T-S diagram for the cooling cycle depicted in figure 1.

valve seat, which is hammered into the seat during the repeated loading. Other samples showed a similar leakage behaviour or did not show leakage at all.

COLD STAGE

Requirements. The requirements for the cold stage are determined by the cooler design of Fig. 1. The associated *T-S* diagram of the cold stage is shown in Fig. 7, the numbered states in the cycle correspond to the numbers in Fig. 1. In the diagram, isobars and isenthalps are given, as well as the enthalpy changes that occur in the counterflow heat exchangers, condenser and evaporator, assuming ideal operation. Under that condition, the cooling power is given by $\dot{m} \cdot \Delta h_{67}$. To obtain the required gross cooling power of 200 mW, an ethylene massflow of 0.5 mg/s is needed. The majority of the enthalpy change Δh_{67} is created during condensation from state 3 to 4. A proper design of the condenser is, therefore, a major requirement so that the two-phase fluid reaches full condensation at state 4.

To obtain a significant cooling power, the thermal losses on the cold stage (conduction and radiation) should be limited, for instance below 50 mW. Because silicon exhibits a very high thermal conductivity, a different material with a low conductivity such as glass should be used for the construction of the counterflow heat exchangers. In constrast, it is attractive to use a high conductivity material (silicon) for the condenser and evaporator to maintain uniform temperatures, independent of the supplied thermal loads.

Design and realization. Fig. 8 shows the design of the cold stage, which is made of three micromachined silicon components with two glass-tube counterflow heat exchangers in between. All three silicon parts are constructed by fusion bonding of two 500 μm thick silicon wafers in which channels and spaces are etched by KOH etching. After processing and separating these silicon samples, the glass tube heat exchangers are glued into the samples, after which integration with a small vacuum flange follows – see Fig. 9. The applied glass tubes are commercially available[12] and have inner/outer diameters of 0.25/0.36 mm and 0.53/0.67 mm, respectively. Two glass support tubes are added parallel to the two counterflow heat exchangers to add more stability to the system.

The left silicon part is called the 'splitter', and makes it possible to supply separate connection lines to the high and low pressure channels of the first counterflow heat exchanger. In the condenser, the high pressure fluid is able to condense in the long meandering channel which

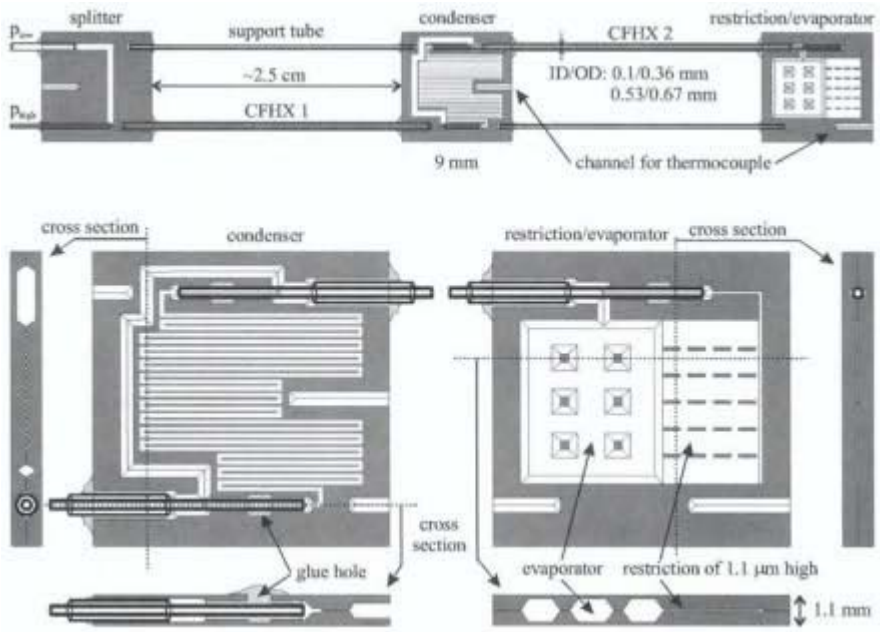

Figure 8. Top: cold stage design, bottom: details and cross sections of the condenser and restriction.

is etched in the silicon. The low pressure fluid returning from the second counterflow heat exchanger directly connects in the condenser to the low pressure annulus of the first counterflow heat exchanger. The high pressure fluid that enters the restriction/evaporator flows through an etched channel to the entrance of the flow restriction, which typically consists of a 4 mm wide, 1 μm shallow channel with a length of about 3 mm. Because the restriction/evaporator is made of a high conductivity material, the high pressure fluid that enters the silicon part easily cools to the low temperature of the evaporator before it enters the flow restriction. This is represented by the dotted extra heat exchanger in Fig. 1 and step 5-5a in the *T-S* diagram of Fig. 7. The low pressure liquid that exits the flow restriction (in state 6a in Fig. 7) is collected in the liquid bath of the evaporator, which connects at the top side to the low pressure annulus of the second counterflow heat exchanger. In the present design, the orientation of the cold stage is important: the low pressure exit of the liquid bath should be oriented vertically upward so that gravity keeps the liquid in the bath and only vapor exits the liquid bath, except when the liquid bath is full. Both the flow restriction and the boiler structure are supported by pillars to prevent excessive bending stresses due to the high gas pressures of 20 bar that may be present. Furthermore, the condenser and the restriction/evaporator contain an etched channel that can be used to insert an external 250 μm thick thermocouple to measure the temperature of these cooler parts.

The high pressure inner glass tubes are glued into the condenser and restriction/evaporator via a so-called 'glue hole', whereas the outer glass tube is glued at the entrance of the sample, see Fig. 8. This construction facilitates a robust separate connection of the high and low pressures.

The surface area of the condenser fits approximately to the surface of a two stage thermoelectric cooler, which is a MI2012T-type fabricated by Marlow Industries[13]. In the same way, a thermal load (some device) can be attached to the restriction/evaporator. In the current design, however, for test purposes a thin film heater is deposited on the restriction/evaporator and on the condenser. This heater can be used to study the behaviour of the cold stage. To limit the radiation load on the cold stage, a gold layer is deposited on both sides of the cooler.

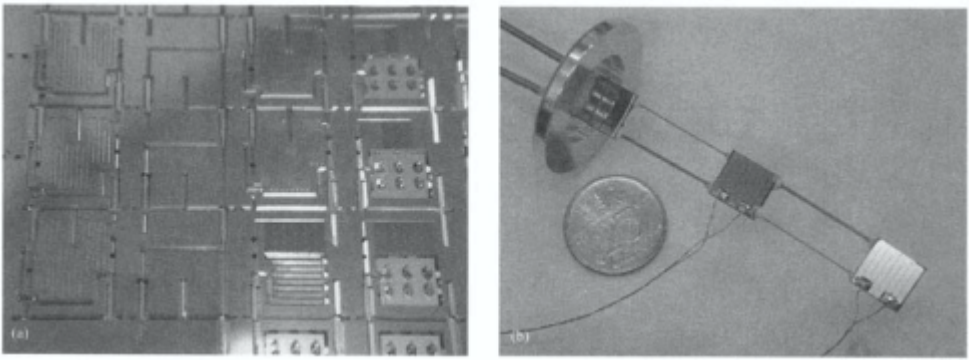

Figure 9. (a) Part of a structured silicon wafer with splitter, condenser and restriction/evaporator samples, (b) Completely assembled cold stage connected to a vacuum flange with wiring to the thin film heaters. The coin (Dutch 25 cents) is 18 mm in diameter.

Experiments. Different versions of the cold stage were characterized in a small vacuum chamber. The high pressure input of a cold stage was connected to an ethylene gas bottle, with a zeolite filter in between to trap possible contaminant gases. A data-acquisition system was used to measure and store the following parameters: the temperatures of the condenser and evaporator, the input powers into the TE-cooler and heaters, the input high pressure and the massflow going into the system and coming out of the system. A typical measurement is depicted in Fig. l0a. The important steps are numbered in the figure and are briefly discussed below.

(1) The high pressure is applied to the cooler and the evaporator cools to a temperature slightly below ambient. The cooling power due to the enthalpy change produced at ambient temperature, Δh_{12}, is too small to overcome the thermal losses and reach lower temperatures. (2) The TE-cooler is started and temperature-controlled at 238 K (-35 °C), 6 K below the condensation temperature at 20 bar. (3) The fluid starts to condense in the condenser. For a short period, the ingoing massflow exceeds the outcoming massflow to compensate for the liquid volume that is now being collected in the condenser. Also, the evaporator starts to cool rapidly because of the increased cooling power of the liquid ethylene. (4) The high pressure fluid now starts to enter the restriction as a liquid, which increases the massflow because of changing fluid density and viscosity. (5) The low pressure boiling temperature is reached and the boiler starts to fill with low pressure liquid. This explains why the ingoing massflow exceeds the outcoming massflow for a while. (6) Because the cooling power exceeds the applied thermal load, two-

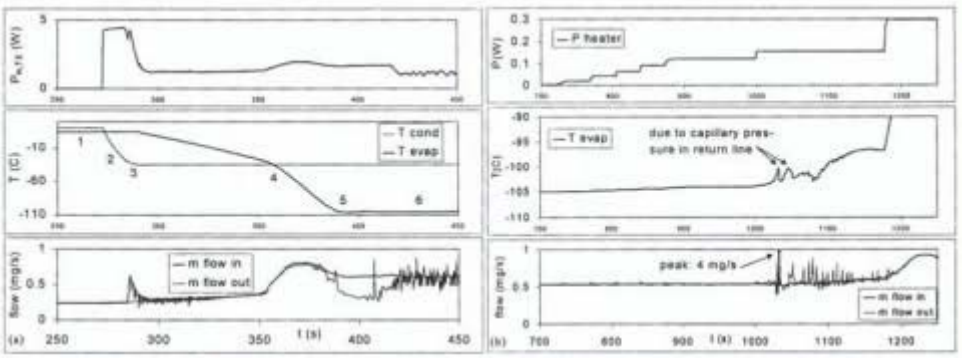

Figure 10. (a) Typical measurement of a start-up of the cold stage, (b) Step-by-step increase of the heater load on the evaporator. At $P_{heater} = 155$ mW, the boiler contents evaporates and T_{evap} starts to rise.

phase fluid exits the evaporator. Capillary effects explain the variations in the outgoing massflow. These variations were dependent on the fraction of the two phases.

In the measurement of Fig. 1 Ob, the thin-film heater on the evaporator is used to determine the net cooling power. During the initial increase of the heat load, a small temperature increase can be observed, which may be explained by the temperature gradient that is present between the wall of the boiler and the boiling liquid. At $P_{heater} = 155$ mW, the liquid in the boiler starts to evaporate, which indicates that the total thermal load (heater + losses) exceeds the cooling power. The first two rapid temperature increases are probably caused by capillary forces, which play an important role because of the small channel dimensions.

CONCLUSIONS

A sorption cooler operating with small stainless steel sorption compressor cells, micromachined check valves and a micromachined cold stage was designed, and elements are constructed and tested. Manufacturing of the sorption cells was simplified by the application of a 250 μm sheathed thermocouple that could also be applied as heater element. The cold stage could reach a stable low temperature of 169 K with a gross cooling power of about 200 mW, provided that no capillary pressure drops occurred in the return line.

ACKNOWLEDGEMENTS

This research is supported by the Dutch Technology Foundation (STW).

REFERENCES

1. Nisenoff, M., Cryocoolers and high temperature superconductors: advancing toward commercial applications, *Cryocoolers 8*, Plenum Press, New York (1995), pp. 913-917.
2. G. Walker and R. Bingham, Micro and nano Cryocoolers: speculation on future development, *Proc. of the 6th Int. Cryocooler Conf.* (1990), pp. 363-375.
3. Burger, J.F., ter Brake, H.J.M., Elwenspoek, M., Rogalla, H., Microcooling: Study on the application of micromechanical techniques, *Cryocoolers 9*, Plenum Press, New York (1997), pp. 687-696.
4. Burger, J.F., *Components for a cryogenic microcooler: a vapor compression cold stage operating on a sorption compressor*, Ph.D. Thesis, Twente University, The Netherlands (2000).
5. Wade, L.A., An overview of the development of sorption refrigeration, *Adv. in Cryogenic Eng.* vol. 37 (1992), pp. 1095-1106.
6. Burger, J.F., Holland, H.J., Wade, L.A., ter Brake, H.J.M., Rogalla, H., Thermodynamic considerations on a microminiature sorption cooler, *Cryocoolers 10*, Plenum Press, New York (1999), pp. 553-564.
7. Gardeniers, J.G.E., Burger, J.F., van Egmond, H., Holland, H.J., ter Brake, H.J.M. and Elwenspoek, M., ZrNi thin films for fast reversible hydrogen pressure actuation, *Proc. of Aktuator 2000*, Bremen, Germany (2000).
8. Omegaclad shielded thermocouple wire, Omega, Inc., Stamford, Connecticut 06907-0047, USA.
9. S. Bard, J. Wu, P. Karlmann, C. Mirate, L. Wade, Component reliability testing of long-life sorption coolers, *Proc. of the 6th Int. Cryocooler Conf.* (1990).
10. J.F. Burger, M.C. van der Wekken, E. Berenschot, H.J. Holland, H.J.M, ter Brake, H. Rogalla, J.G.E. Gardeniers and M. Elwenspoek, High pressure check valve for application in a miniature cryogenic sorption cooler, *Proc of IEEE MEMS 99* (1999).
11. C. Gui, *Direct wafer bonding with chemical mechanical polishing*, Ph.D. Thesis, Twente University (1998).
12. Supelco/Sigma-Aldrich Corp., Bellefonte, PA, USA.
13. Marlow Ind. Inc., 10451 Vista Park Road, Dallas, Texas 75238-1645, USA.